Synthesis, characterization and kinetics of thermal decomposition of 2'-amino-1-benzyl-6'-(1H-indol-3-yl)-2-oxospiro[indoline-3,4'-pyran]-3',5'-dicarbonitrile under non isothermal condition in nitrogen atmosphere.

[1]G.Nalini, [2]N.Jayachandramani, [3]R.Suresh, [4]P.Thirumurugan, [5]V.Thanikachalam, [6]G. Manikandan

[1,2]Department of Chemistry, Pachaiyappa's College ,Chennai-600 030, India.
[3]Department of Chemistry, Presidency College, Chennai-600 005, India.
[4]Department of Chemistry, Organic Chemistry Division, CSIR-CLRI, Chennai-600 020, India.
[5,6]Department of Chemistry, Annamalai University,Annamalainagar-608 002,India.
Email: sureshradhakrishnan@gmail.com

[Received:1st March 2016; Revised:30th May 2016; Accepted:1st June 2016; Available online:10th June 2016]

Abstract: A spirooxindole compound, namely 2'-amino-1-benzyl-6'-(1H-indol-3yl)-2-oxospiro[indoline-3,4'-pyran]-3',5'-dicarbonitirile [AB$_z$IOIPD] was synthesized and characterized by microanalysis, FT-IR, mass specta and NMR (^{1}H and ^{13}C) techniques. The thermal decomposition of the compound was studied by thermogravimetric analysis under dynamic nitrogen atmosphere at different heating rates of 10,15,20 and 30 K min^{-1}. The kinetic parameters were calculated using model fitting (Coats–Redfern, CR) and model–free methods (Friedman, Kissinger–Akahira–Sunose, KAS and Flynn–Wall-Ozawa, FWO). The decomposition process of AB$_z$IOIPD followed a single step mechanism as evidenced from the data. Existence of compensation effect is noticed for the decomposition of AB$_z$IOIPD. Invariant kinetic parameters are consistent with the average values obtained by Friedman and KAS inconversional methods.

Keywords: Spirooxindole, dispirooxindole - pyrrolidine, 2'-Amino-1-benzyl- 6'-(1H-indol-3-yl)-2-oxospiro[indoline-3,4'-pyran]-3',5'-dicarbonitrile, thermal decomposition, model fitting , model free methods

I. INTRODUCTION

The spirooxindole system is the core structure of a variety of medicinal agents and natural products[1,2]. The spirooxindole derivatives have been described with different biological activities, ranging from [3,4] anti-tumor, anti-imflammatry, analgesic, antimicrobial [5], anti-HIV, antimalarial and as antipyretic agents. [6] Compounds such as 5-[(Indol-2-on-3-yl)methyl]-2,2-dimethyl-1,3-dioxane-4,6-diones and spirocyclopropyloxindole derivatives have been reported to behave as poliovirus and rhinovirus and potential aldose reductase inhibitors. Spiro-pyrrolidinyl oxindoles [7] have been extensively studied as potent inhibitors of p53-MDM2 interaction, finally leading to the identification of MI-888, which could achieve rapid, complete and durable tumor regression in xenograft models of human cancer advanced preclinical research for cancer therapy. Spirooxindole systems are of great interest in modern organic, medicinal, and natural product chemistry. This type of framework forms a core structure of many alkaloids with promising pharmacological activity, such as horsfiline, gelsemine, mitraphylline and spirotryprotatins A,B [8]. Novel dispirooxindole-pyrrolidine derivatives have been synthesized through 1,3-dipolar cycloaddition of an azomethine ylide generated from isatin and sarcosine with the dipolarphile 3-(1H-indole-3-yl)-3-oxo-2-(2-oxoindolin-3-ylidene) propanenitrile and also spiro compound of acenaphthenequinone obtained by the same optimized reaction condition. The synthesized compounds were evaluated for their antimicrobial activity and all the compounds showed significant activity. Non-isothermal decomposition kinetics of chitosan [9], chitin [10], cephalosporins [11], procaine and benzocaine [12] and theobromine [13] were studied in detail and appropriate kinetic models were proposed.

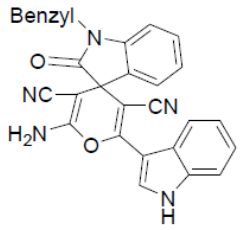

Figure 1: Structure of AB$_z$IOIPD

In this paper, we report the synthesis and characterization of 2'-amino-6'-(1H-indol-3-yl)-2-oxospiro[indoline-3,4'-pyran] -3',5'-dicarbonitrile (Fig.1)[14] and its thermal decomposition under non-isothermal condition in dynamic nitrogen atmosphere. The thermal decomposition of AB$_z$IOIPD spiroderivative compound was studied by using TG/DTG and DTA methods. In this report, the kinetic

and thermodynamic parameters were computed by using model-fitting and model free- methods.

II. EXPERIMENTAL

2.1. Materials

1-Benzylindoline-2,3-dione, malononitrile, 3-cyanoacetyl indole and DMSO-d_6 were purchased from Aldrich Chemicals. Acetic anhydride and other reagents were procured from S.D.Fine Chemicals and were used as received.

2.2. Instruments

Elemental analyses were performed at Central Leather Research Institute (CLRI), Chennai, India. IR measurements was done using Perkin Elmer Spectrometer RXI FT-IR. The ^{1}H and ^{13}C NMR spectra were recorded in DMSO-d_6 using TMS as internal standard with JEOL ECA-500MH$_z$ and Bruker 400-500MH$_z$ high resolution NMR spectrometer. The mass spectrum was recorded using Electrospray Ionisation Method with Thermo Finnigan mass spectrometer. Melting points were determined in capillary tubes and are uncorrected. Analytical TLC was performed on precoated plastic sheets of silica gel G/UV-254 of 0.2 mm thickness. The simultaneous TGA curves were obtained with the thermal analysis system model Perkin Elemer TAC7/DX (Thermal Analysis Controller TAC-7). The TG analyses of AB$_z$IOIPD were carried out under dynamic nitrogen atmosphere (100 ml min^{-1}) in an Iron pan with the sample at the heating rates of 10,15,20 and 30 K min^{-1} from 30 to 850°C. TGA was recorded at Indian Institute of Technology, Chennai, India. The kinetic parameters E_a and A were calculated using Microsoft Excel Software. The sample temperature, controlled by thermocouple, did not exhibit any systematic deviation from the preset linear temperature programme.

2.3. Synthesis of 2'-amino-1-benzyl-6'-(1H-indol-3yl)-2-oxospiro[indoline-3,4'-pyran]-3',5'-dicarbonitirile

To a stirred solution of 1-benzylindoline-2,3-dione (0.294 g, 2 mmol), malononitrile (0.122 g, 2 mmol), and 3-cyanoacetyl indole (0.368 g, 2 mmol) in methanol (20 mL), triethyl amine (20 mol %) was added and stirring was continued. On completion, the reaction mixture was poured into crushed ice and the precipitate formed was filtered, dried and purified by column chromatography to afford the pure product. The isolated product was further purified by recrystallisation in ethanol and the yield of the product was 92 %.

Elemental analysis: Calculated % for $C_{29}H_{19}N_5O_2$: C 74.19 H 4.08 N 14.92. Found: C 74.22 H 4.09 N 14.94. Pale brown solid; mp 222-225 ^{o}C; R_f 0.48 (40% AcOEt/Petroleum ether); IR (KBr): 1156, 1354, 1535, 1610, 1665, 1706, 2203, 2370, 2928, 3321, 3437 cm^{-1}; ^{1}H NMR (500 MHz, DMSO-d_6): δ 4.99 (q, J = 11.68 Hz, 2H, Ar-CH_2), 6.91 (d, J = 7.65 Hz, 1H, Ar-H), 7.14 (t, J = 6.9 Hz, 1H, Ar-H), 7.19 (t, J = 8.4 Hz, 1H, Ar-H), 7.23-7.30 (m, 5H, Ar-H), 7.37 (d, J = 7.65 Hz, 2H, Ar-H), 7.46 (d, J = 7.65 Hz, 1H, Ar-H), 7.52 (d, J = 7.65 Hz, 1H, Ar-H), 7.72 (s, 2H,-NH_2), 8.00 (d, J= 8.4 Hz, 1H, Ar-H), 8.20 (s, 1H, Ar-H), 12.11 (brs, 1H,-NH); ^{13}C NMR (125 MHz, DMSO-d_6)**:** δ 43.8, 50.2, 54.5, 81.2, 105.5, 110.4, 113.0, 117.7, 117.9, 121.9, 122.1, 123.5, 124.3, 124.9, 125.6, 127.5, 128.0, 129.1, 130.6, 131.6, 136.0, 136.5, 142.5, 158.6, 160.5, 176.4; MS (EI): m/z 470.07 [M^++H^+] .

III THEORETICAL BACKGROUND

3.1. Model fitting method

There are numerous non-isothermal model-fitting methods, and the most popular one is the Coats-redfern [10] method which has been successfully used for studying the kinetics of dehydration and decomposition of different solid substances [15,16]. The kinetic parameters can be derived from the modified Coats and Redfern Eq. (1)

$$\ln\left[\frac{g(\alpha)}{T^2}\right] = \ln\left(\frac{AR}{\beta E_a}\left[1-\left[\frac{2RT}{E_a}\right]\right)\right) \cong \ln\left(\frac{AR}{\beta E_a}\right) - \frac{E_a}{RT}, \quad (1)$$

where g(α) is an integral form of the conversion function (α), the expression of which depends on the kinetic model of the occurring reaction. If the correct g(α) function is used, a plot of ln [g(α)/T^2] against l/T should give a straight line from which the values of the activation energy, E_a and the pre-exponential factor, A can be calculated.

2. Model free methods

Friedman method [17] is a differential method and is one of the first used isoconversional methods. The model in the logarithmic form is given as

$$\frac{d\alpha}{dt} = A\exp\left(\frac{-E_a}{RT}\right) f(\alpha) \quad (2)$$

$$\ln\left[\beta\frac{d\alpha}{dT}\right] = \ln\left[A_\alpha f(\alpha)\right] - \frac{E_{a,\alpha}}{RT_\alpha} \quad (3)$$

The plots of ln (βdα/dT) Vs 1/T (Eq. (3)), at each α gives E_a from the slope of the plot.

The isoconversional integral method suggested independently by Horowitz et.al and Friedman [18,19], is based on the equation:

$$\ln\beta = \ln\left[\frac{0.0048\,AE_a}{g(\alpha)\,R}\right] - 1.0516\frac{E_a}{RT} \quad (4)$$

and Kissinger–Akahira–Sunose (KAS) equation [25,26] (Eq. (5)) is

$$\ln\left(\beta/T^2\right) = \ln\left[\frac{AE_a}{g(\alpha)\,R}\right] - \frac{E_a}{RT} \quad (5)$$

Values of apparent activation energies for the decomposition of AB$_z$IOIPD at different values of α can be calculated. According to these equations, the reaction

mechanism and shape of g(α)function do not affect the values of the activation energies of the decomposition stages.

3.3. Invariant kinetic parameters (IKP) method

The invariant kinetic parameters are obtained by the method of Lesnikovich and Levchik. The straight lines obtained for the plots of ln A_β Vs E_β for several constant heating rates should intersect at a point [20] which corresponds to the true values of activation energy and pre-exponential factor and they are named invariant kinetic parameters (E_{inv}, A_{inv}) which are evaluated using the super correlation relation Eq. (6)

$$a_\beta = \ln A_{inv} - b_\beta E_{inv} \qquad (6)$$

Plot of a_β Versus b_β gives a straight line [21], the values of E_{inv} and ln A_{inv} are calculated from the slope and intercept of the plot respectively.

3.4. Thermodynamic parameters

The kinetic parameters, energy of activation (E_a) and pre-exponential factor (A) are obtained from Kissinger single point [19, 22, 23] kinetic method which uses the Eq. (7):

$$\ln\left(\beta / T_m^2\right) = -\frac{E_a}{RT_m} + \ln\left(\frac{AR}{E_a}\right) \qquad (7)$$

Where T_m is temperature that corresponds to the maximum of $d\alpha/dT$. This 'model-free' kinetic method can be applied with a reasonable approximation without being limited to n-order kinetics,[26], providing a single E_a value for each reaction step. For this reason, it is often defined as a Kissinger single point method. The reaction proceeds under conditions where thermal equilibrium is always maintained, then a plot of $\ln\left(\frac{\beta}{T_m^2}\right)$ versus $\frac{1}{T_m}$ gives a straight line with a slope equal to $-E_a/R$.

Based on the values of activation energy and pre-exponential factor for the decomposition stage, the values of $\Delta S^{\neq}$, $\Delta H^{\neq}$ and $\Delta G^{\neq}$ for the formation of activated complex from the reactant were calculated based on the following [23-26] equations:

$$\Delta S^{\neq} = R \ln \frac{Ah}{e\chi k_B T_p} \qquad (8)$$

Since

$$\Delta H^{\neq} = E_a - RT_p \qquad (9)$$

$$\Delta G^{\neq} = \Delta H^{\neq} - T_p \Delta S^{\neq} \qquad (10)$$

IV. RESULTS AND DISCUSSION

4.1. Non-isothermal TGA

The themograms of pure AB_zIOIPD recorded in a dynamic nitrogen atmosphere at different heating rates of 10, 15, 20 and 30 K min^{-1} are presented in Figures 2A and 2B. They show two distinct endothermic peaks due to melting and decomposition. The thermal decomposition process of ABIOIPD in four stages is observed from the TGA curves. The decomposition process for first stage starts at 150°C and ends at 225°C with the mass loss of 17.33%.The second stage decomposition starts at 255°C and ends at 348°C with the mass loss of 9.58%.The third stage of decomposition starts at 348°C and ends at 550°C with the mass loss of 11.99%. The fourth stage decomposition starts at 550°C and ends at 850°C with the mass of 16.75%.

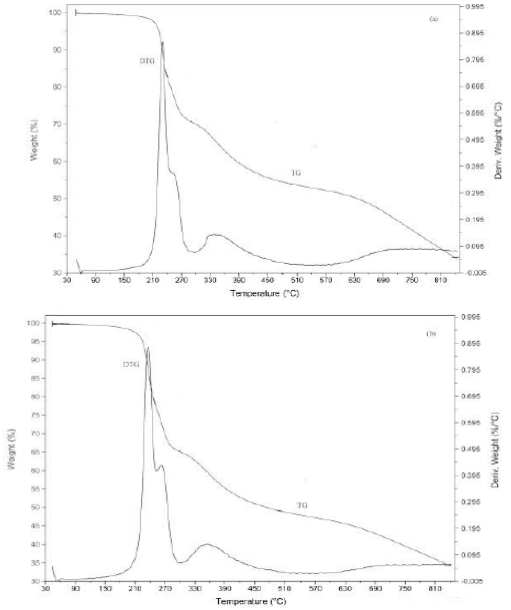

Figure 2A. TG and DTG Curves of AB_zIOIPD at (a) 10$min^{-1}$and (b) 15 Kmin^{-1} heating rates in nitrogen atmosphere.

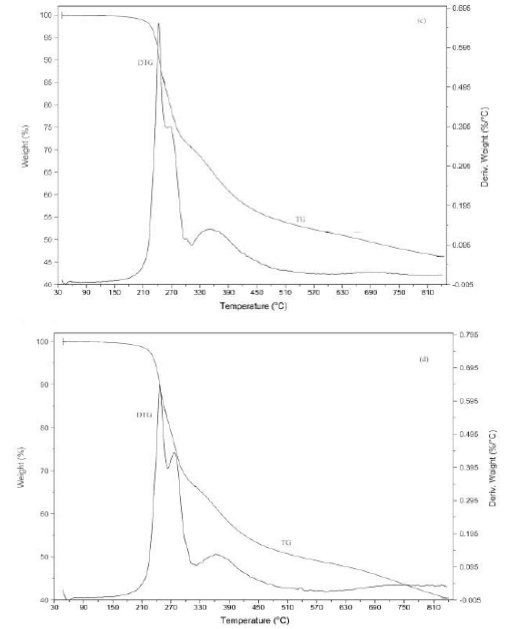

Figure 2B . TG and DTG Curves of AB_zIOIPD at (c) 20 K min^{-1} and (d) 30 K min^{-1} heating rates in nitrogen atmosphere.

4.2 Model-free analysis

The non-isothermal decomposition kinetics of AB_zIOIPD is first analyzed by model-free methods viz., Friedman ,Kissinger- Akahira-Sunose and Flynn-Wall-Ozawa. Tables 1- 4 show the variation of apparent activation energy E_a, as a function of extent of conversion α, for the decomposition of AB_zIOIPD. E_a value increases slightly in the conversion range of $0.12 \leq \alpha \leq 0.98$ for all the stages. It was pointed out [18] that when E_a changes with α, the Friedman and KAS isoconversional methods lead to close values of E_a for all the stages. The applied isoconversional methods do not suggest a direct way for evaluating either the pre-exponential factor (A) or the analytical form of the reaction model f(α), for the investigated decomposition process of AB_zIOIPD.

For the first stage decomposition of AB_zIOIPD, the values of energy of activation corresponding to the different values of α for the decomposition process obtained by Friedman, KAS and FWO methods are listed in Table 1 (Figure 3).It is seen that E_a value depends upon the extent of conversion α. The average value of E_a is 231.37 ± 0.72 kJ/mol (KAS method). From Figure 3(Table 1), it is evident that the values of activation energy obtained by Friedman and FWO methods (229.04 ± 0.86 kJ/mol, Friedman; 227.98 ± 0.41 kJ/mol, FWO) are slightly less than that of KAS method.

Table 1. Temperatures corresponding to the degree of conversion at different heating rates for AB_zIOIPD compound (stage-I)

α	Heating Rate				E_a (kJ/(mol)		
	10 K/min	15 K/min	20 K/min	30 K/min	Friedman method	KAS method	FWO method
0.12	482.91	485.16	487.42	491.76	236.37	231.46	227.77
0.14	486.24	488.67	490.95	495.22	234.25	232.79	229.09
0.16	488.91	491.18	493.47	497.94	233.05	232.20	228.57
0.18	490.74	493.03	495.3	499.84	232.59	232.15	228.56
0.20	492.07	494.53	496.8	501.26	231.26	232.71	229.10
0.22	493.41	495.7	498.02	502.61	230.54	231.83	228.29
0.24	494.4	496.7	499.17	503.63	229.48	231.96	228.43
0.26	495.23	497.71	500.0	504.56	228.67	231.97	228.45
0.28	496.02	498.37	500.8	505.34	228.61	231.55	228.07
0.30	496.72	499.04	501.5	506.06	229.84	231.31	227.85
0.32	497.38	499.7	502.24	506.74	229.16	231.30	227.85
0.34	497.88	500.37	502.76	507.31	230.79	231.74	228.28
0.36	498.38	500.88	503.24	507.84	229.31	231.51	228.07
0.38	498.88	501.37	503.68	508.37	228.17	231.06	227.65
0.40	499.26	501.71	504.1	508.75	228.19	230.98	227.58
0.42	499.85	502.38	504.88	509.37	228.69	231.41	228.00
0.44	500.28	502.88	505.4	509.83	229.22	231.60	228.19
0.46	500.68	503.32	505.87	510.25	230.24	231.72	228.31
0.48	501.04	503.84	506.36	510.65	230.87	232.29	228.85
0.5	501.45	504.29	506.91	511.07	229.42	232.36	228.93
0.52	502.03	504.79	507.56	511.64	228.41	232.10	228.68
0.54	502.44	505.25	507.97	512.09	228.36	231.98	228.58
0.56	502.75	505.57	508.28	512.42	228.98	231.86	228.47
0.58	502.91	505.73	508.43	512.59	229.91	231.80	228.42
0.60	503.17	506.0	508.67	512.87	230.10	231.71	228.33
0.62	503.34	506.21	508.9	513.05	229.16	231.78	228.41
0.64	503.81	506.67	509.41	513.53	230.44	231.72	228.35
0.66	504.22	507.18	509.78	514.00	229.46	231.69	228.33
0.68	504.78	507.67	510.45	514.54	230.29	231.63	228.28
0.70	505.0	507.89	510.72	514.76	230.27	231.61	228.26
0.72	505.91	508.81	511.54	515.74	229.05	231.21	227.91
0.74	506.28	509.16	511.91	516.12	229.98	231.12	227.82
0.76	506.53	509.49	512.18	516.4	230.79	231.28	227.98
0.78	506.89	509.8	512.49	516.77	229.71	231.09	227.80
0.80	507.41	510.29	513.15	517.28	228.28	230.98	227.71
0.82	508.08	510.84	513.8	517.94	229.31	230.72	227.47
0.84	508.52	511.28	514.2	518.41	229.24	230.57	227.34
0.86	509.41	512.22	515.0	519.38	228.44	230.26	227.06
0.88	510.27	512.97	515.88	520.23	229.96	230.11	226.93
0.90	511.1	513.99	516.86	521.13	228.84	230.53	227.34
0.92	511.65	514.64	517.53	521.72	226.43	230.53	227.35

0.94	512.3	515.47	518.43	522.42	222.81	230.36	227.19
0.96	513.11	516.32	519.38	523.29	217.67	229.30	226.21
0.98	513.83	517.2	520.24	524.11	213.21	228.26	225.22
				Mean	229.04±0.86	231.37±0.72	227.98±0.41

Table 2. Temperatures corresponding to the degree of conversion at different heating rates for AB_zIOIPD compound (stage-II).

A	**Heating Rate**				**E_a (kJ/(mol)**		
	10 K/min	**15 K/min**	**20 K/min**	**30 K/min**	**Friedman method**	**KAS method**	**FWO method**
0.12	519.40	522.00	524.62	529.63	257.94	231.36	228.27
0.14	520.06	522.64	525.24	530.25	255.35	232.78	229.63
0.16	520.56	523.17	525.80	530.73	253.09	234.03	230.82
0.18	521.00	523.66	526.39	531.15	252.49	235.29	232.03
0.20	521.68	524.34	526.94	531.83	251.55	236.07	232.78
0.22	522.28	525.01	527.51	532.44	251.70	237.08	233.75
0.24	522.76	525.51	528.10	532.90	252.86	238.15	234.77
0.26	523.21	526.01	528.65	533.34	253.61	239.17	235.75
0.28	523.92	526.68	529.31	534.03	253.70	240.03	236.57
0.30	524.31	527.18	529.81	534.43	252.67	241.01	237.52
0.32	524.86	527.84	530.32	535.01	253.74	241.84	238.32
0.34	525.36	528.38	531.00	535.49	253.78	242.80	239.24
0.36	525.83	528.98	531.50	535.99	252.03	243.53	239.94
0.38	526.37	529.52	532.17	536.51	251.91	244.15	240.53
0.40	526.86	530.19	532.66	537.05	251.27	244.80	241.16
0.42	527.35	530.69	533.30	537.52	252.21	245.30	241.65
0.44	527.88	531.36	533.84	538.09	251.55	245.80	242.13
0.46	528.39	532.03	534.52	538.61	252.30	246.39	242.69
0.48	528.78	532.50	535.03	539.00	251.89	246.66	242.96
0.50	529.34	533.18	535.66	539.58	252.24	247.03	243.31
0.52	529.87	533.59	536.20	540.08	253.59	247.49	243.76
0.54	530.39	534.06	536.83	540.57	252.12	247.68	243.95
0.56	531.05	534.57	537.50	541.19	253.29	248.08	244.35
0.58	532.05	535.35	538.41	542.16	252.74	248.55	244.81
0.60	532.78	536.09	539.33	542.86	251.85	248.56	244.82
0.62	533.70	536.86	540.22	543.76	251.36	248.70	244.97
0.64	534.11	537.45	540.70	544.21	252.86	249.29	245.54
0.66	534.89	538.05	541.35	544.98	253.93	249.63	245.87
0.68	535.58	539.00	542.06	545.76	252.21	250.42	246.64
0.70	536.41	539.73	542.94	546.57	251.74	250.40	246.64
0.72	537.05	540.57	543.61	547.28	252.00	250.87	247.09
0.74	537.80	541.41	544.48	548.05	251.51	250.89	247.12
0.76	538.81	542.55	545.60	549.10	252.01	250.99	247.24
0.78	539.71	543.48	546.60	550.01	252.18	250.97	247.23
0.80	540.95	544.65	547.63	551.35	251.42	251.15	247.41
0.82	542.12	545.83	548.65	552.61	252.29	251.26	247.54
0.84	543.52	546.97	550.00	553.98	253.69	251.62	247.90
0.86	544.88	548.30	551.51	555.34	252.48	251.62	247.93
0.88	546.30	550.12	553.17	556.86	251.24	252.02	248.33
0.90	548.10	552.30	555.24	558.74	252.41	252.07	248.41
0.92	550.22	554.30	557.24	560.98	249.63	251.83	248.22
0.94	552.21	556.65	559.59	563.09	243.63	250.15	246.65
0.96	554.45	559.33	561.95	565.60	236.68	247.41	244.08
0.98	557.12	561.91	564.42	568.60	232.02	244.49	241.35
				Mean	251.52±0.49	245.67±0.36	242.08±0.89

Table 3. Temperatures corresponding to the degree of conversion at different heating rates for AB_zIOIPD compound (stage-III).

	Heating Rate				**E_a (kJ/(mol)**		
A	**10 K/min**	**15 K/min**	**20 K/min**	**30 K/min**	**Friedman method**	**KAS method**	**FWO method**
0.12	589.22	591.99	594.79	599.54	408.14	297.11	291.88
0.14	592.55	595.18	597.98	602.14	406.66	323.50	317.02
0.16	595.72	598.53	601.19	604.88	405.61	345.24	337.73
0.18	598.22	600.88	603.71	607.06	404.31	357.96	349.86

0.20	600.55	603.39	606.24	609.20	404.98	368.48	359.90
0.22	602.88	605.73	608.58	611.41	403.12	376.03	367.11
0.24	605.38	608.22	610.95	613.87	403.38	382.71	373.51
0.26	607.71	610.59	613.30	616.17	402.59	387.23	377.84
0.28	610.21	613.10	615.83	618.65	402.92	390.93	381.39
0.30	612.54	615.27	618.01	620.98	402.92	393.69	384.06
0.32	614.87	617.61	620.41	623.31	403.28	395.76	386.07
0.34	617.21	619.96	622.75	625.68	404.13	397.70	387.94
0.36	619.71	622.47	625.25	628.22	404.74	399.41	389.61
0.38	622.05	624.82	627.61	630.60	404.67	400.59	390.77
0.40	624.38	627.17	629.97	632.98	403.98	401.34	391.52
0.42	626.88	629.68	632.35	635.58	404.05	402.14	392.33
0.44	629.22	632.03	634.84	637.94	403.74	402.35	392.56
0.46	631.89	634.55	637.20	640.72	402.05	402.18	392.44
0.48	634.39	636.89	639.74	643.22	402.37	401.84	392.15
0.50	636.90	639.75	642.46	645.86	403.22	403.34	393.62
0.52	639.56	642.26	644.96	648.58	404.17	403.22	393.55
0.54	642.40	645.11	647.69	651.52	404.90	403.45	393.82
0.56	645.06	647.62	650.41	654.19	403.10	403.06	393.49
0.58	647.89	650.63	653.21	657.16	404.88	403.86	394.29
0.60	650.90	653.65	655.76	660.31	404.29	402.87	393.40
0.62	654.07	656.50	658.94	663.45	403.38	402.71	393.30
0.64	657.40	659.51	662.18	666.74	404.87	402.24	392.91
0.66	660.56	662.86	665.33	670.05	403.77	403.00	393.68
0.68	664.07	666.38	668.96	673.64	404.47	403.63	394.34
0.70	667.73	670.23	672.41	677.47	404.75	403.43	394.20
0.72	671.57	673.92	676.11	681.36	404.30	402.50	393.38
0.74	675.57	677.94	680.15	685.47	403.23	402.60	393.54
0.76	680.07	682.13	684.75	689.95	404.80	403.08	394.07
0.78	684.40	686.49	688.80	694.41	403.19	401.63	392.76
0.80	689.41	691.01	694.04	699.31	403.46	402.31	393.49
0.82	693.85	696.03	698.34	704.09	403.07	404.23	395.38
0.84	699.25	701.57	703.82	709.69	404.13	404.37	395.60
0.86	704.95	707.10	709.64	715.48	404.61	404.33	395.66
0.88	711.02	712.79	716.45	721.48	403.32	406.07	397.40
0.90	718.25	720.33	723.97	729.05	404.60	406.66	398.08
0.92	725.09	728.06	730.76	736.51	399.52	406.25	397.81
0.94	731.85	735.24	737.54	743.72	394.63	401.51	393.41
0.96	737.56	741.45	744.96	749.60	389.97	403.11	395.02
0.98	745.44	749.84	752.72	758.15	385.32	395.67	388.07
				Mean	402.99±0.04	393.30±0.60	384.32±0.71

Table 4. Temperatures corresponding to the degree of conversion at different heating rates for AB_zIOIPD compound (stage-IV).

	Heating Rate				**E_a (kJ/(mol)**		
α	**10 K/min**	**15 K/min**	**20 K/min**	**30 K/min**	**Friedman method**	**KAS method**	**FWO method**
0.12	858.86	862.32	865.95	872.40	538.51	479.60	469.68
0.14	872.70	876.56	879.93	886.00	537.69	511.11	499.86
0.16	884.50	888.64	892.41	897.82	536.09	524.69	512.95
0.18	895.39	898.87	902.85	908.75	534.27	528.07	516.34
0.20	905.07	908.92	912.29	918.82	532.94	530.21	518.52
0.22	913.08	916.80	920.72	926.94	532.61	531.65	520.02
0.24	920.75	924.68	928.63	934.88	531.78	532.06	520.53
0.26	927.76	931.72	935.54	942.13	531.86	531.46	520.08
0.28	934.26	938.26	942.45	948.79	530.08	531.52	520.24
0.30	939.93	944.13	948.17	954.71	530.28	531.26	520.09
0.32	945.94	949.66	954.07	960.73	531.99	530.41	519.37
0.34	951.44	955.19	959.46	966.42	531.55	530.26	519.32
0.36	956.61	960.73	964.86	971.85	530.51	531.38	520.47
0.38	961.78	966.09	970.08	977.24	531.56	531.52	520.68
0.40	966.96	970.95	974.97	982.50	531.33	530.02	519.34
0.42	971.96	975.98	980.02	987.64	532.97	530.64	520.01
0.44	976.80	981.01	984.74	992.70	531.29	530.39	519.85
0.46	981.46	985.70	989.62	997.48	532.82	531.46	520.94

0.48	986.47	990.23	994.50	1002.47	532.17	530.38	520.00
0.50	991.14	995.09	999.23	1007.34	531.90	531.00	520.66
0.52	995.98	1000.12	1003.77	1012.41	531.07	529.95	519.74
0.54	1000.82	1004.82	1008.66	1017.33	532.74	530.29	520.14
0.56	1005.32	1009.34	1013.38	1021.96	531.05	531.00	520.89
0.58	1010.33	1014.37	1018.10	1027.13	532.91	530.01	520.03
0.60	1014.83	1018.90	1022.81	1031.76	531.99	531.04	521.08
0.62	1019.67	1023.76	1027.70	1036.75	532.10	531.10	521.21
0.64	1024.50	1028.45	1032.42	1041.68	531.91	530.22	520.45
0.66	1029.18	1032.98	1036.96	1046.44	532.54	529.51	519.86
0.68	1034.02	1037.85	1041.69	1051.43	531.42	529.08	519.53
0.70	1038.69	1042.71	1046.57	1056.30	530.71	530.34	520.80
0.72	1043.36	1047.23	1051.12	1061.06	530.98	529.29	519.87
0.74	1048.36	1052.10	1055.84	1066.15	531.47	527.84	518.58
0.76	1053.20	1056.95	1060.73	1071.13	530.25	528.21	519.01
0.78	1057.87	1061.65	1065.44	1075.94	531.01	528.65	519.50
0.80	1062.70	1066.34	1070.16	1080.85	531.30	528.03	518.99
0.82	1067.37	1071.37	1075.04	1085.77	531.96	530.28	521.20
0.84	1072.17	1076.07	1079.76	1090.67	532.42	529.76	520.78
0.86	1077.22	1080.76	1084.95	1095.73	532.04	530.17	521.25
0.88	1082.05	1085.62	1089.93	1100.72	531.25	530.74	521.88
0.90	1086.72	1090.65	1094.98	1105.66	532.44	533.29	524.37
0.92	1091.73	1095.34	1099.93	1110.73	530.00	531.31	522.57
0.94	1096.90	1100.37	1105.99	1115.97	529.54	533.97	525.18
0.96	1101.73	1105.23	1110.95	1121.01	527.74	532.64	524.00
0.98	1106.91	1110.43	1116.26	1126.43	523.99	530.61	522.15
Mean					531.80±0.32	528.78±0.28	518.68±0.46

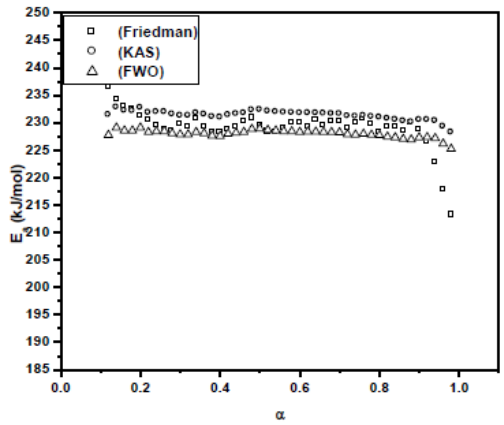

Figure 3. Ea versus α plot for the decomposition of AB_zIOIPD under non-isothermal condition (stage I)

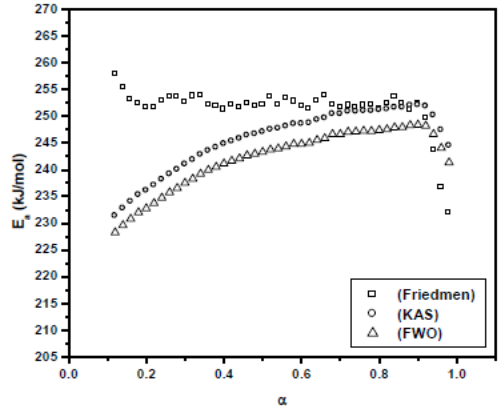

Figure 4. Ea versus α plot for the decomposition of ABzIOIPD under non-isothermal condition (stage II)

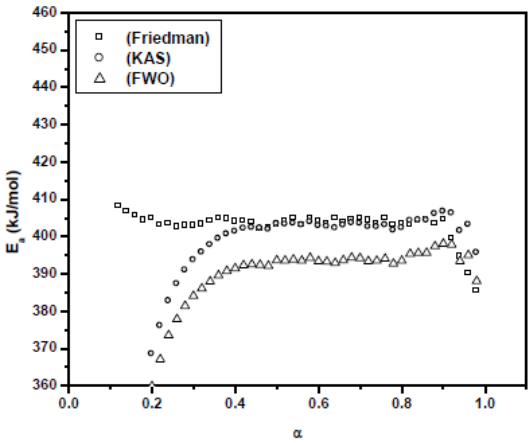

Figure 5. E_a versus α plot for the decomposition of AB_zIOIPD under non- isothermal condition (stage III)

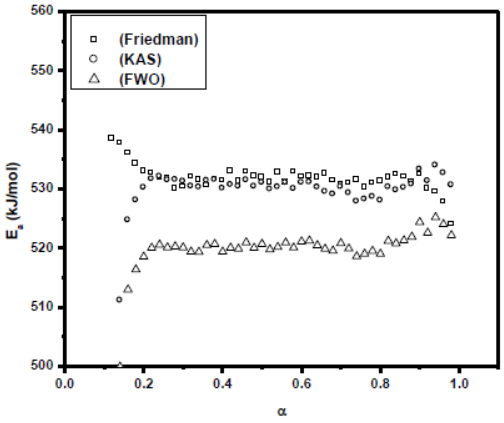

Figure 6. Ea versus α plot for the decomposition of ABzIOIPD under non- isothermal condition (stage IV)

For stage II the variation of E_a with α for the decomposition is shown in Figure 4 (Table 2). The average value of E_a is 251.52 ± 0.49 kJ/mol (Friedman method) .From Table 2, it is evident that the Friedman method activation energy is higher than the values of activation energy obtained by KAS (E_a = 245.67 ± 0.36 kJ/mol) and FWO (E_a = 242.08 ± 0.89 kJ/mol) methods.

For stage III , the values of apparent activation energies obtained by Friedman and KAS methods are higher than that of FWO method. The average values of E_a in the range $0.12 \leq \alpha \leq 0.98$ were 402.99 ± 0.04 kJ/mol (Friedman), 393.30 ± 0.60 kJ/mol (KAS),and 384.32 ± 0.71 kJ/mol (FWO)(Table 3; Figure 5). Form Table 3, it is evident that the Friedman method and KAS methods gave higher values of activation energy than the FWO method.

For stage IV, the values of apparent activation energies obtained by Friedman and KAS methods are higher than that of FWO method. The average values of E_a in the range $0.12 \leq \alpha \leq 0.98$ were 531.80 ± 0.32 kJ/mol (Friedman), 528.78 ± 0.28 kJ/mol (KAS),and 518.68 ± 0.46 kJ/mol (FWO)(Table 4 ; Figure 6). From the average values of E_a for each stage, the rate of decomposition is found to depend upon the nature of the intermediate formed during the decomposition. The fourth stage is slower than the other stages of decomposition. The higher value of activation energy for stage IV than the other stages indicates that the intermediate compounds are thermally more stable and hence the decomposition process is slow.

4.3 Model-fitting analysis

After carrying out model-free analysis, model–fitting can be done in the conversion region where apparent activation energy is approximately constant where a single model may fit. The non-isothermal kinetic data of AB_zIOIPD at $0.12 \leq \alpha \leq 0.98$ where model-free analysis indicates approximately constant activation energy, were then fitted in to each of the 15 models listed in Tables 5, 6, 7 and 8 ,for stages 1, 2, 3 and 4 respectively. As shown in Tables 5, 6, 7 and 8,for the applied method [20], Arrherius parameters (E_a, lnA) for decomposition process, exhibit strong dependence on the reaction model chosen.

Table 5. Arrhenius parameters for nonisothermal decomposition of compound AB_zIOIPD (stage-I) at various heating rates.

Kinetic model	β = 10 K/min			β = 15 K/min			β = 20 K/min			β = 30 K/min		
	E_a (kJ/mol)	lnA	r	E_a (kJ/mol)	lnA	r	E_a (kJ/mol)	lnA	r	E_a (kJ/mol)	lnA	r
P2	82.84	18.58	-0.986	80.73	18.34	-0.989	78.59	17.98	-0.989	82.02	19.06	-0.987
P3	52.39	10.94	-0.985	50.97	10.90	-0.988	49.52	10.74	-0.988	51.79	11.61	-0.985
P4	37.25	7.03	-0.983	36.17	7.09	-0.987	35.08	7.03	-0.987	36.76	7.79	-0.983
F1	270.68	64.83	-0.997	263.77	63.21	-0.998	257.28	61.60	-0.998	268.38	64.13	-0.998
F2	407.80	98.61	-0.991	396.80	95.83	-0.990	387.12	93.30	-0.990	404.32	97.00	-0.991
F3	579.45	140.68	-0.980	563.22	136.44	-0.978	549.53	132.76	-0.977	574.47	137.95	-0.980
D1	373.00	95.93	-0.989	364.49	93.80	-0.991	355.85	91.57	-0.991	370.22	94.68	-0.989
D2	408.75	96.78	-0.993	399.01	94.31	-0.995	389.35	91.78	-0.995	405.50	95.22	-0.993
D3	476.47	111.93	-0.996	464.81	108.92	-0.998	453.58	105.94	-0.998	472.65	109.94	-0.997
D4	431.03	100.76	-0.994	420.66	98.11	-0.996	410.48	95.43	-0.996	427.59	99.06	-0.995
A2	131.17	30.82	-0.997	127.69	30.19	-0.998	124.43	29.51	-0.998	129.94	30.99	-0.997
A3	84.57	19.26	-0.997	82.24	18.97	-0.998	80.05	18.60	-0.998	83.70	19.73	-0.997
A4	61.41	13.42	-0.997	59.65	13.29	-0.998	58.00	13.07	-0.998	60.72	14.03	-0.997
R2	217.41	50.94	-0.995	212.03	49.75	-0.997	206.78	48.50	-0.997	215.56	50.58	-0.995
R3	202.50	47.51	-0.993	197.54	46.44	-0.995	192.63	45.28	-0.995	200.77	47.24	-0.993

Table 6. Arrhenius parameters for nonisothermal decomposition of compound AB_zIOIPD (stage-II) at various heating rates.

Kinetic model	β = 10 K/min			β = 15 K/min			β = 20 K/min			β = 30 K/min		
	E_a (kJ/mol)	lnA	r	E_a (kJ/mol)	lnA	r	E_a (kJ/mol)	lnA	r	E_a (kJ/mol)	lnA	r
P2	56.40	10.98	-0.926	55.15	10.99	-0.933	54.25	10.98	-0.935	57.60	12.09	-0.923
P3	34.60	5.68	-0.914	33.75	5.80	-0.921	33.13	5.89	-0.924	35.34	6.78	-0.910
P4	23.76	2.91	-0.900	23.11	3.09	-0.907	22.64	3.22	-0.910	24.28	4.00	-0.895
F1	196.66	44.01	-0.978	192.33	43.13	-0.981	189.37	42.51	-0.983	201.03	45.23	-0.976
F2	304.63	69.37	-0.995	297.51	67.71	-0.997	292.71	66.55	-0.998	311.71	70.73	-0.995
F3	440.56	101.07	-0.999	429.86	98.41	-1.000	422.70	96.57	-0.999	451.08	102.61	-0.999
D1	266.52	66.47	-0.943	261.61	65.37	-0.948	258.07	64.54	-0.951	272.09	67.68	-0.940
D2	292.40	64.51	-0.953	286.59	63.16	-0.959	282.50	62.17	-0.961	298.65	65.73	-0.951
D3	345.03	75.35	-0.968	337.89	73.63	-0.972	332.96	72.39	-0.974	352.55	76.63	-0.966
D4	309.70	67.07	-0.959	303.45	65.60	-0.964	299.09	64.53	-0.966	316.36	68.31	-0.957
A2	93.89	20.17	-0.975	91.70	19.92	-0.979	90.20	19.73	-0.981	95.99	21.32	-0.974
A3	59.57	12.00	-0.973	58.09	11.96	-0.977	57.08	11.92	-0.979	60.91	13.13	-0.971
A4	42.51	7.83	-0.970	41.39	7.89	-0.975	40.61	7.92	-0.976	43.47	8.95	-0.968
R2	155.14	33.48	-0.960	151.87	32.89	-0.964	149.59	32.47	-0.966	158.50	34.64	-0.957
R3	143.60	31.00	-0.953	140.61	30.50	-0.958	138.51	30.13	-0.960	146.68	32.15	-0.950

Table 7. Arrhenius parameters for nonisothermal decomposition of compound AB_zIOIPD (stage-III) at various heating rates.

Kinetic model	β = 10 K/min			β = 15 K/min			β = 20 K/min			β = 30 K/min		
	E_a (kJ/mol)	lnA	r	E_a (kJ/mol)	lnA	r	E_a (kJ/mol)	lnA	r	E_a (kJ/mol)	lnA	r
P2	11.15	-1.71	-0.856	11.48	-1.23	-0.860	11.60	-0.93	-0.857	11.16	-0.67	-0.853
P3	3.80	-4.04	-0.640	4.01	-3.56	-0.654	4.07	-3.25	-0.652	3.75	-3.00	-0.630
P4	0.15	-7.90	-0.043	0.29	-6.81	-0.082	0.33	-6.40	-0.091	0.07	-7.54	-0.021
F1	57.91	8.71	-0.983	59.01	9.28	-0.983	59.55	9.63	-0.983	58.28	9.70	-0.983
F2	93.38	16.29	-0.998	95.07	16.95	-0.998	95.98	17.34	-0.998	94.04	17.25	-0.998
F3	137.96	25.57	-0.998	140.39	26.34	-0.998	141.77	26.77	-0.999	138.98	26.48	-0.998
D1	88.60	21.53	-0.958	90.10	22.16	-0.958	90.80	22.52	-0.957	89.24	22.51	-0.957
D2	90.48	13.66	-0.962	92.12	14.32	-0.962	92.89	14.68	-0.961	91.08	14.61	-0.962
D3	107.85	15.85	-0.977	109.78	16.54	-0.977	110.72	16.92	-0.976	108.58	16.78	-0.976
D4	96.19	13.38	-0.968	97.93	14.04	-0.968	98.75	14.41	-0.967	96.83	14.32	-0.967
A2	23.53	1.55	-0.974	24.06	2.05	-0.974	24.30	2.36	-0.973	23.63	2.58	-0.973
A3	12.05	-1.21	-0.955	12.38	-0.74	-0.956	12.53	-0.43	-0.954	12.06	-0.17	-0.953
A4	6.34	-2.90	-0.911	6.58	-2.42	-0.915	6.68	-2.11	-0.912	6.31	-1.85	-0.907
R2	44.23	4.98	-0.963	45.10	5.53	-0.963	45.51	5.85	-0.962	44.48	5.99	-0.962
R3	40.41	4.39	-0.954	41.22	4.93	-0.954	41.59	5.25	-0.952	40.64	5.40	-0.953

Table 8. Arrhenius parameters for nonisothermal decomposition of compound AB_zIOIPD (stage-IV) at various heating rates.

Kinetic model	β = 10 K/min			β = 15 K/min			β = 20 K/min			β = 30 K/min		
	E_a (kJ/mol)	lnA	r	E_a (kJ/mol)	lnA	r	E_a (kJ/mol)	lnA	r	E_a (kJ/mol)	lnA	r
P2	17.15	-2.16	-0.976	17.39	-1.72	-0.977	17.60	-1.42	-0.977	17.03	-1.15	-0.976
P3	5.90	-4.46	-0.910	6.04	-4.03	-0.914	6.16	-3.72	-0.916	5.73	-3.46	-0.906
P4	0.31	-8.03	-0.145	0.40	-7.37	-0.186	0.47	-6.92	-0.216	0.12	-7.97	-0.055
F1	86.05	7.83	-0.999	86.89	8.30	-0.999	87.66	8.64	-0.999	86.22	8.75	-0.999
F2	135.70	14.78	-0.986	136.96	15.28	-0.986	138.14	15.64	-0.986	136.06	15.63	-0.986
F3	197.72	23.23	-0.970	199.51	23.76	-0.970	201.20	24.16	-0.970	198.32	23.99	-0.970
D1	135.56	21.68	-0.995	136.80	22.18	-0.995	137.90	22.54	-0.995	136.13	22.58	-0.995
D2	137.34	12.93	-0.997	138.67	13.43	-0.998	139.84	13.80	-0.998	137.75	13.78	-0.998
D3	162.00	14.85	-1.000	163.53	15.36	-1.000	164.91	15.74	-1.000	162.51	15.66	-1.000
D4	145.46	12.56	-0.999	146.85	13.06	-0.999	148.10	13.43	-0.999	145.90	13.40	-0.999
A2	34.76	0.88	-0.999	35.15	1.32	-0.999	35.50	1.63	-0.999	34.71	1.87	-0.999
A3	17.63	-1.82	-0.998	17.87	-1.39	-0.998	18.08	-1.08	-0.998	17.51	-0.81	-0.998
A4	9.11	-3.48	-0.996	9.28	-3.05	-0.996	9.42	-2.74	-0.997	8.96	-2.47	-0.996
R2	66.67	4.33	-0.999	67.35	4.79	-0.999	67.96	5.12	-0.999	66.77	5.28	-0.999
R3	61.23	3.80	-0.997	61.87	4.26	-0.997	62.43	4.58	-0.997	61.31	4.76	-0.997

4.4 Invariant Kinetics Parameters (IKP) analysis

Criado and Morales [27] reported that almost any α=α(T) or (dα/dt) (T) experimental curve may be correctly described by several conversion functions. The use of an intergral or differential model-fitting method leads to different values of the activation parameters. Although obtained with high accuracy the values change with different heating rates and among conversion functions.

Lesnikovich and Levchik [28] suggested that correlating these values by the apparent compensation effect, $\ln A = a_\beta + b_\beta E_a$,one obtains the compensation effect parameters a_β and b_β, which strongly depend on the heating rates (β) as well as on the considered set of conversion functions. The straight lines of ln A verus E_a for four constant heating rates should intersect at a point (isoparamertric point) which corresponds to the true values of the activation energy and pre-exponential factor. These were named as invariant kinetic parameters.

The invariant kinetic parameters method was applied to the data calculated for the heating rates of 10, 15, 20 and 30 $Kmin^{-1}$. The evaluation of the kinetic parameters was performed using Coats-Redfern method. For these kinetic models in the range $0.12 \leq \alpha \leq 0.98$ for AB_zIOIPD for all the stages, the straight lines corresponding to Coats-Redfern method is characterized by correlation coefficient values close to unity.

For several groups of apparent activation parameters, obtained by different kinetic models, we tried to establish the best correlation (r→1), a better resolution in determining the invariant kinetics parameters and the closet value to the mean isoconversional activation energies. [29-31].

For stage I for AKM, the plot of lnA versus E_a has the highest correlation coefficient and is a straight line (Table 9; Figure 7). The invariant kinetic parameters, E_{inv} = 231.37 ± 72 kJ/mol for AKM and $\ln A_{inv}$ = 54.65 (Table 9) are obtained with r = 0.993 (Figure 7). For these group, the invariant activation energy is almost equal to 231.72 kJ/mol compared to KAS and Friedman

methods (229.04 ± 0.86 kJ/mol, Friedman; 231.72 ± 0.5 kJ/mol, KAS; 227.98 ± 0.41 kJ/mol, FWO).

Table 9. Compensation effect parameter for several combinations of kinetic models for AB_zIOIPD (Stage-I)

β (K/min)	AKM			AKM-{F1 ; F2 ; F3 ; D1 ; D4 }			AKM-{A2 ; R3 }		
	a_β A/min	b_β/mol/J	r	a_β A/min	b_β/mol/J	r	a_β A/min	b_β/mol/J	r
10	0.243	-1.527	0.998	0.239	-1.154	0.999	0.238	-1.326	0.999
15	0.242	-1.160	0.998	0.237	-0.814	0.999	0.2372	-0.960	0.999
20	0.241	-0.914	0.998	0.236	-0.569	0.999	0.236	-0.715	0.999
30	0.239	-0.478	0.998	0.234	-0.132	0.999	0.234	-0.279	0.999

Table 10. Compensation effect parameter for several combinations of kinetic models for AB_zIOIPD (Stage-II)

β (K/min)	AKM			AKM-{F2 ; D1 ; D3 ; D4 }			AKM-{D2 }		
	a_β A/min	b_β/mol/J	R	a_β A/min	b_β/mol/J	r	a_β A/min	b_β/mol/J	r
10	-2.019	0.232	0.997	-2.260	0.232	0.999	-2.324	0.234	0.999
15	-1.652	0.231	0.997	-1.890	0.231	0.999	-1.956	0.233	0.999
20	-1.393	0.229	0.997	-1.630	0.230	0.999	-1.697	0.232	0.999
30	-0.936	0.227	0.997	-1.177	0.228	0.999	-1.240	0.230	0.999
β (K/min)	AKM-{F1 ; A2}			AKM-{R2 ; R3 }					
	a_β A/min	b_β/mol/J	R	a_β A/min	b_β/mol/J	r			
10	-2.407	0.234	0.999	-2.353	0.234	0.999			
15	-2.039	0.233	0.999	-1.985	0.233	0.999			
20	-1.779	0.232	0.999	-1.726	0.232	0.999			
30	-1.323	0.230	0.999	-1.222	0.230	0.999			

Table 11. Compensation effect parameter for several combinations of kinetic models for AB_zIOIPD (stage-III)

β (K/min)	AKM			AKM-{P4 ; D1 }			AKM-{P3 ; D4 ; A2 }		
	a_β A/min	b_β/mol/J	r	a_β A/min	b_β/mol/J	r	a_β A/min	b_β/mol/J	r
10	-4.651	0.218	0.971	-4.013	0.201	0.992	-3.960	0.204	0.993
15	-4.117	0.215	0.972	-3.559	0.200	0.992	-3.537	0.203	0.993
20	-3.806	0.214	0.973	-3.269	0.199	0.992	-3.248	0.202	0.994
30	-3.70	0.217	0.969	-2.917	0.199	0.991	-2.890	0.202	0.993
β (K/min)	AKM-{ F1 ; D3 ; A3}			AKM-{F2 ; F3 }			AKM-{R3 }		
	a_β A/min	b_β/mol/J	r	a_β A/min	b_β/mol/J	r	a_β A/min	b_β/mol/J	r
10	-4.325	0.213	0.998	-3.870	0.196	0.999	-3.948	0.195	0.999
15	-3.899	0.212	0.998	-3.440	0.195	0.999	-3.515	0.194	0.999
20	-3.611	0.211	0.998	-3.151	0.194	0.999	-3.226	0.194	0.999
30	-3.253	0.210	0.998	-2.799	0.193	0.999	-2.876	0.193	0.999

Table 12. Compensation effect parameter for several combinations of kinetic models for AB_zIOIPD stage-IV)

β (K/min)	AKM			AKM-{F2 ; D1 ; D3 ;D4 }			AKM-{D2 }		
	a_β A/min	b_β/mol/J	r	a_β A/min	b_β/mol/J	r	a_β A/min	b_β/mol/J	r
10	-5.086	0.142	0.966	-4.252	0.139	0.999	-4.252	0.139	0.999
15	-4.633	0.141	0.966	-4.036	0.139	0.999	-3.840	0.138	0.999
20	-4.317	0.140	0.967	-3.752	0.138	0.999	-3.555	0.138	0.999
30	-4.198	0.142	0.963	-3.384	0.138	0.999	-3.190	0.137	0.999
β (K/min)	AKM-{F1 ; A2 }								
	a_β A/min	b_β/mol/J	r						
10	-4.092	0.138	0.999						
15	-3.683	0.137	0.999						
20	-3.683	0.137	0.999						
30	-3.029	0.136	0.999						

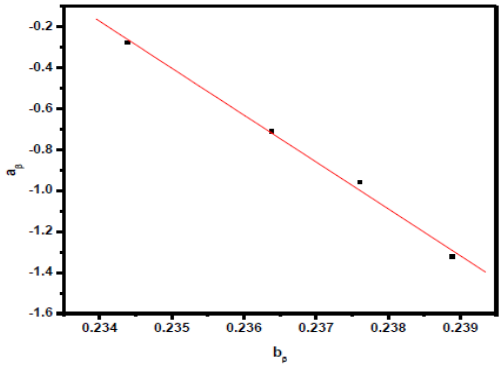

Figure 7. Supercorrelation (compensation effect parameters) plot for the best combination of kinetic models (Stage-I)

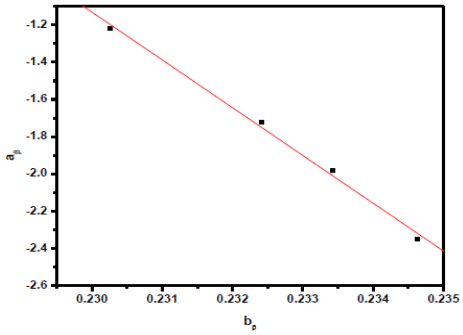

Figure 8. Supercorrelation (compensation effect parameters) plot for the best combination of kinetic models (Stage-II)

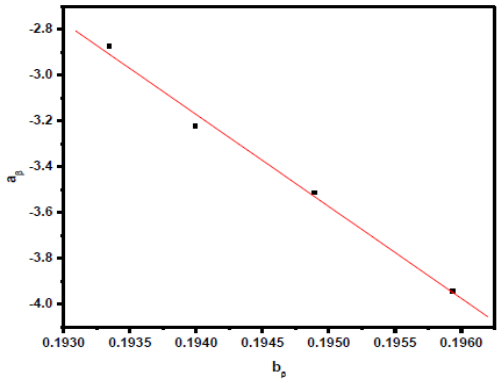

Figure 9. Supercorrelation (compensation effect parameters) plot for the best combination of kinetic models (Stage-IV)

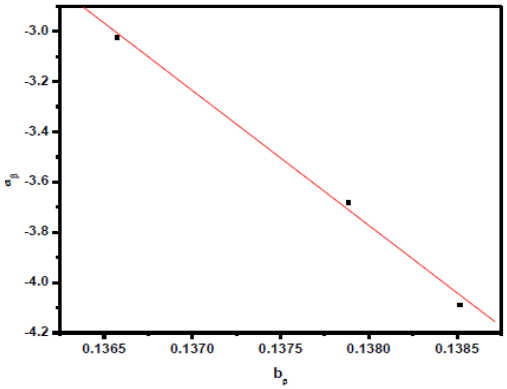

Figure 10. Supercorrelation (compensation effect parameters) plot for the best combination of kinetic models (Stage-III)

For stage II, a better resolution in determing the invariant kinetic parameters (Table 10), and the correlation coefficient in Table 10 show a good agreement of all kinetic models. The efficiency of IKP method is strongly revealed by AKM-{ R2; R3} (Figure 8) and even by AKM (all kinetic models) which comprises all the best-fitting function that makes it a more powerful method. The invariant activation energy is 256.15 kJ/mol, which is close to Friedman method. The invariant kinetic parameters are E_{inv} = 256.15 kJ/mol and ln A_{inv} = 57.78 obtained with r = 0.997.

For third stage of AKM- {R3}, the plot of lnA versus E_a has the highest correlation coefficient (r = 0.996) (Table 11; Figure 9). Depending upon the choice of kinetic models, the compensation effect parameters are obtained with different accuracies, their values and the derived invariant activation parameters varying substantially. For AKM- {R3}, the invariant kinetic parameters are 401.78 kJ/mol and ln A_{inv} = 74.77 obtained with r = 0.996 (Table 11).For these groups, the invariant activation energy is slightly above 6 units (E_a = 439.35 ± 0.22 kJ/mol) and 12 units (E_a = 433.97 ± 0.57 kJ/mol) obtained by Friedman and FWO methods.

For fourth stage of AKM – {F1;A2}, the plot of lnA versus E_a has the highest correlation (r = 0.996) (Table 12; Figure 10) coefficient and energy of activation coincides with that obtained by Friedman method. For AKM – {F1;A2}, the invariant kinetic parameters are 537.09 kJ/mol and ln A_{inv} = 70.34 obtained with r = 0.996.

4.5. Determination of kinetic models

The most suitable kinetic model for the decomposition process of AB_zIOIPD is F1. By introducing the derived reaction model g(α) = -ln(1-α), the following equation is obtained.

$$-\ln(1-\alpha) = \frac{AE_a}{R\beta} p(x) \qquad (11)$$

The plots of -ln(1–α) against E_a p(x)/Rβ at the different heating rates are shown in Figure 11.The activation energy for stage I, E_a = 231.37 kJ/mol and the frequency factor was found to be 5.422 x 10^{23}(ln A= 54.65). The obtained value of lnA is in good agreement with values obtained by KAS isoconversional intercept. The most suitable kinetic model for stage is F2 (second order). By introducing the derived reaction model g(α) = $(1-\alpha)^{-1}$ -1, the following equation is obtained.

$$(1-\alpha)^{-1}-1 = \frac{AE_a}{R\beta} p(x) \qquad (12)$$

The plot of $(1-\alpha)^{-1}$ -1 against $E_a p(x)/R\beta$ at the different heating rates are shown in Figure 12. The activation energy for stage II, E_a = 251.52 kJ/mol, the pre-

exponential frequency factor A =1.240 x 10^{25} (ln A = 57.78).

The most suitable kinetic model is F3 for stages III and IV as confirmed by introducing the derived reaction model g(α) = 0.5 [(1-α)$^{-2}$ -1], when the following equation is obtained [32, 33].

$$0.5\,[(1-\alpha)^{-2}-1] = \frac{AE_a}{R\beta}\,p(x) \qquad (13)$$

The plots of 0.5 [(1–α)$^{-2}$–1] against $E_a p(x)/R\beta$ at the different heating rates are shown in Figures 13 and 14. The activation energy E_a = 402.99 kJ/mol and frequency factor for stage III is 2.966 x 10^{32} (lnA= 74.77) and the activation energy E_a = 531.80 kJ/mol and the frequency factor for stage IV is 3.534 x 10^{30} (lnA =70.43) as determined by IKP method.

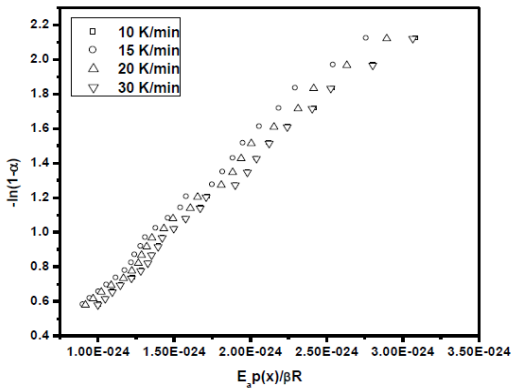

Figure 11. Determination of A value by plotting -ln(1-α) against E_a p(x)/βR for the decomposition of AB_zIOIPD at different heating rates (β) (stage-I)

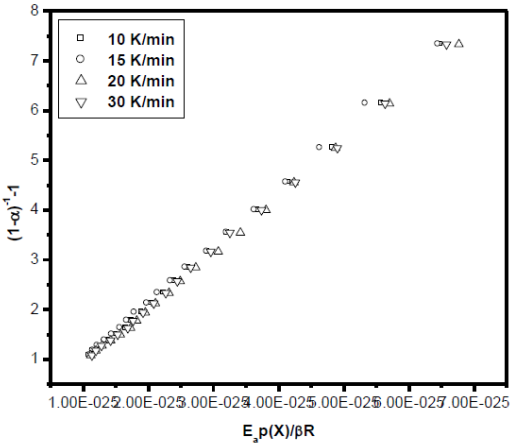

Figure 12. Determination of A value by plotting [(1-α)$^{-1}$-1] against E_a p(x)/βR for the decomposition of AB_zIOIPD at different heating rates (β) (stage-II

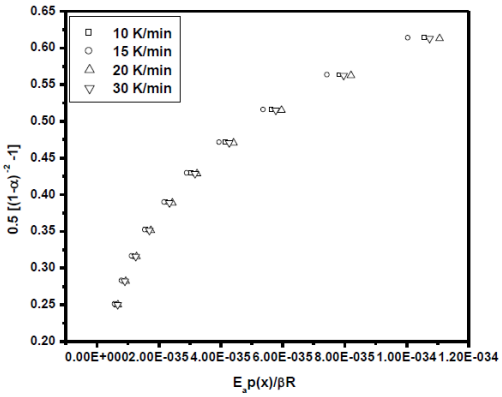

Figure 13. Determination of A value by plotting 0.5[(1-α)$^{-2}$-1] against E_a p(x)/βR for the decomposition of AB_zIOIPD at different heating rates (β) (stage-III)

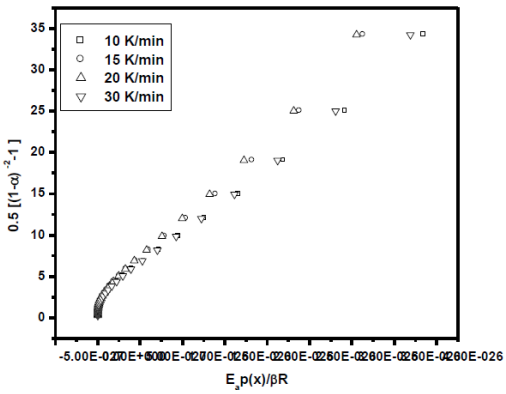

Figure 14. Determination of A value by plotting 0.5[(1-α)$^{-2}$-1] against E_a p(x)/βR for the decomposition of AB_zIOIPD at different heating rates (β) (stage-IV)

4.6. Thermodynamic parameters

From the DTG curves, the peak temperatures for AB_zIOIPD are 491.91, 540.37, 653.06 and 915.45 K. These peak temperatures are used to evaluate single point kinetic parameters [34,35]. The obtained values are 184.77, 118.68, 218.64 and 439.71 K for stages I , II ,III and IV respectively. The thermodynamic parameters, $\Delta S^{\neq}$, $\Delta H^{\neq}$ and $\Delta G^{\neq}$ were calculated at the peak temperature T_m in the DTG curves for the corresponding stage [36,37] since the temperature characterizes the higher rate of decomposition and therefore, is an important parameter.

Table 13. Values of kinetic and thermodynamic parameters for the thermal decomposition of AB_zIOIPD in nitrogen atmosphere.

Parameter	Stage I	Stage II	Stage III	Stage IV
Ea/kJmol^{-1}	184.77	118.68	218.64	439.71
ln A	45.01	25.68	39.71	57.21
$\Delta G\neq$/kJmol^{-1}	122.72	138.62	166.77	235.91
$\Delta H\neq$/kJmol^{-1}	180.65	114.13	213.16	432.05
$\Delta S\neq$/JK^{-1}mol^{-1}	116.84	44.76	70.41	213.12
r	0.987	0.994	0.993	0.991

As can be seen from Table 13, the value of $\Delta S^{\neq}$ for the decomposition is positive for all the stages. It means

that the corresponding activated complexes were with lesser degrees of arrangement than the initial state. The positive values of $\Delta H^{\neq}$ and $\Delta G^{\neq}$ show that they are connected with absorption of heat and are non-spontaneous processes [38]. The obtained E_a values coincide with invariant parameters.

V. CONCLUSION

The compound chosen for study decomposed in four stages with absorption of heat. The 'model' for the decomposition is F1 for stage I and F2 for stage II and F3 for stages III and IV. The thermal stability of AB_zIOIPD in the fourth stage is high and the corresponding energy of activation is also high compared to the other stages. The rate of the first stage decomposition is higher than the other stages because of lower energy of activation.

VI. ACKNOWLEDGMENTS

The authors thank Dr.P.T Perumal, Organic Chemistry Division, CSIR- Central Leather Research Insititute, Chennai for the fruitful suggestions and The Head, Indian Institute of Technology, SAIF, Chennai for TGA–DTA measurements.

REFERENCES

[1] R.T.Brown, "Indoles, The Monoterpenoid Indole Alkaloids", Wiley: New York, NY., 25, 1983.

[2] J.Ed.ApSimon, "The total synthesis of natural products", Wiley Interscience, New York, 5, 264, 1983.

[3] T.L. Pavlovska, Gr.R. Redkin, V.V .Lipson and D. V. Atamanuk, "Molecular diversity of spirooxindoles. Synthesis and biological activity", Cross Mark, Springer International Publishing Switzerland, 2015.

[4] M.M.Santos Maria, " Recent advances in the synthesis of biologically active Spirooxindoles", Tetrahedron Lett., 70, pp. 9735-9757, 2014.

[5] G.Bhaskar, Y.Arun, C.Balachandran, C.Saikumar, P.T.Perumal, "Synthesis of novel spirooxindole derivatives by one pot multicomponent reaction and their antimicrobial activity", European Journal of Medicinal Chemistry, 51, pp. 79-91, 2012.

[6] W.G.Rajeswaran, R.B.Labroo, E.A.Cohen, "Synthesis of 5-[(Indol-2-on-3-yl)methyl]-2,2-dimethyl-1,3- dioxane-4,6-diones and Spirocyclopropyloxindole Derivatives. Potential Aldose Reductase Inhibitors**"**, J. Org. Chem. 64, pp. 1369-1371, 1999**.**

[7] Yu.Bin,Yu. De-Quan and Liu. Hong-Min, "Spirooxindoles: Promising scaffolds for anticancer agents", European Journal of Medicinal Chemistry, 97, pp. 673-698, 2015.

[8] R.Sakhuja, S. Siva, L. Khnna,S. Khurana and S.C. Jain,"Design and synthesis of spiro[indole-thiazolidine]spiro[indolepyrans] as antimicrobial agents", Bioorg.Med.Chem. Lett., 21, pp. 5465-5469, 2011.

[9] Yu.Fuchao,R. Huang,Ni. Hangchen,F. Juan, Y. Shengjiao and L. Lin, "Three-component stereoselective synthesis of spirooxindole derivatives", Green Chem.,15, pp. 453-462, 2013.

[10] Y.Arun,G. Bhaskar,C. Balachandran,S. Ignacimuthu and P.T. Perumal,"Facile one-spot synthesis of novel dispirooxindole-pyrrolidine derivatives and their antimicrobial and anticancer acitivty against A549 human lung adenocarcinoma cancer cell line", Bioorg. Med. Chem. Lett., 23, pp. 1839-1845, 2013.

[11] V. Georgieva,D. Zvezdova and L.Vlaev,"Non-isothermal kinetics of thermal degradation of chitosan", Chem.Cent. J., 6:81, 2012.

[12] V.Georgieva, D. Zvezdova and L. Vlaev,"Non-isothermal kinetics of thermal degradation of chitin", J.Therm.Anal.calorim., 111, pp. 763-771, 2013.

[13] A. Fulias,G. Vlase,T. Vlase, C. Soica,A. Heghes,M. Craina and I. Ledeti, "Comparative kinetic analysis on thermal degradation of some cephalosporins using TG and DSC data", Chem.Cent. J, **7**:70, 2013.

[14] A.Fulias, G. Vlase, C. Grigorie, I. Ledeti, P. Albu, M.Bilanin and T. Vlase, "Thermal behaviour Studies of procaine and benzocaine", J.Therm.Anal.calorim., 113, pp. 265-271, 2013.

[15] T.L.Kamel, "Non-isothermal decomposition kinetics of theobromine in nitrogen atmosphere", Eur.J.Chem., 6(2) , pp. 199-203, 2015.

[16] A.Nandakumar**,** P**.** Thirumurugan**,** P.T**.**Perumal**,**P. Vembu, N.M. Ponnuswamy and P.Ramesh, "One-pot multicomponent synthesis and antimicrobial evaluation of 2' -(indol-3-yl)-2-oxospiro indoline-3,4' -pyran) derivatives**"**, Bioorg.Med.Chem.Lett., 20, pp. 4252-4258, 2010.

[17] **A.W.**Coats and J.P. Redfern**,** "Kinetic parameters from thermo gravimetric data**"**, Nature (London)**.,** 201, pp. 68**,** 1964.

[18] H.H.Horowitz and G. Metzger, "A new analysis of thermogravimetric traces", Anal. Chem., 35, pp. 1464–1468, 1963.

[19] H. L. Friedman, "Kinetics of thermal degradation of charfoaming plastics from thermogravimetry-application to a phenolic resin", Polym. Sci., C 6, pp. 183–195, 1963.

[20] J. H. Flynn and L. A. Wall, "General treatment of the thermogravimetric of polymers", J. Res. Natl. Bur. Stand. , A 70, pp. 487–523, 1966.

[21] T.Ozawa, "A new method of analyzing thermogravimetric data", Bull. Chem. Soc. Jpn., 38, pp. 1881–1886, 1965.

[22] T. Akahira and T.Sunose, "Joint convention of four electrical institutes", Res. Report CHIBA Inst. Technol., 16, pp. 22–31, 1971.

[23] H. E Kissinger, "Reaction kinetics in differential thermal analysis", Anal.chem., 29, pp. 1702-1706, 1957.

[24] A. I. Lesnikovich and S. V. Levchik**,** "Isoparametric kinetic relations of chemical transformation in condensed substances**",** J.Therm. Anal.**,** 30, pp. 237-262, 1985.

[25] H.J Flynn, "The 'temperature integral' – its use and abuse", Thermochim.Acta., 300, pp. 83–92, 1997.

[26] E.H. Kissinger, "Variation of peak temperature with heating rate in differential thermal analysis", J. Res. Natl. Bur. Stand. , 57, pp. 217-221, 1956.

[27] D. J. Whelan, R. J .Spear and R.W. Read, "The thermal decomposition of some primary explosives as studied by differential scanning calorimetry", Thermochim. Acta., 80, pp. 149-163, 1984.

[28] F.H. Cordes, "Preexponential factors for solid-state thermal decomposition", J. Phys. Chem., 72, pp. 2185–2189, 1968.

[29] C.H.Bamford and C.F.H. Tipper, "Comprehensive chemical kinetics, Reactions in the Solid State", 22, pp. 1-340, 1980.

[30] J.A. Malek, "Computer program for kinetic analysis of nonisothermal thermoanalytical data", Thermochim. Acta., 136, pp. 337–346, 1989.

[31] S. Vyazovkin, and W.Linert, "False isokinetic relationships found in the nonisothermal decomposition of solids", Chem.Phys., 193, pp. 109-108, 1995.

[32] J.M.Criado and J. Morales, "Defects of thermogravimetric analysis for discerning between first-order reactions and those taking place through the Avrami-Erofeev□ s mechanism", Thermo chim.Acta.,16, pp. 382-387, 1976.

[33] A.I. Lesnikovich and S.V. Levchik, "Variation of peak temperature with heating rate in differential thermal analysis", J.Therm.Anal., 27, pp. 89-94, 1983.

[34] S.V.Vyazovkin and A.I. Lesnikovich, "Estimation of the Pre-exponential Factor in the Isoconversional Calculation of Effective Kinetic Parameters", Thermochim. Acta., 128, pp. 297-300, 1998.

[35] P.Budrugeac and E. Segal, "Applicability of the Kissinger equation in thermal analysis", J. Therm. Anal. Calorim., 88, pp. 703-707, 2007.

[36] A. Pratap**,**T.L.S. Rao**,** Lad and H.D.Dhaurandhar**,** " Isoconversional vs Modelfitting Methods**",** J.Therm.Anal.calorim.**,** 89**,** pp**.** 399-405**,** 2007.

[37] J. Malek**,** "The kinetic analysis of non-isothermal data**",** Thermochim.Acta.**,** 200**,** pp**.** 257-269**,** 1992.

[38] J.M.Criado, L.A.Perez-Maqueda and P.E.Sanchez-Jimenez, "The dependence of the preexponential factor on temperature", J.Therm. Anal. Calorim., 82, pp. 671-675, 2005.

◈◈◈